

Article

Serpentinite from Moeche (Galicia, North Western Spain). A Stone Used for Centuries in the Construction of the Architectural Heritage of the Region

José Nespereira ¹, Rafael Navarro ², Serafín Monterrubio ^{1,2}, Mariano Yenes ³
and Dolores Pereira ^{2,3,*} 

¹ Department of Geology, University of Salamanca, Avd. Requejo 33, 49022 Zamora, Spain; jnj@usal.es (J.N.); seramp@usal.es (S.M.)

² CHARROCK Research Group. University of Salamanca, Plaza de los Caídos s/n, 37008 Salamanca, Spain; rafanavarro74@gmail.com

³ Department of Geology, University of Salamanca, Plaza de los Caídos s/n, 37008 Salamanca, Spain; myo@usal.es

* Correspondence: mdp@usal.es

Received: 1 April 2019; Accepted: 10 May 2019; Published: 12 May 2019



Abstract: Serpentinites are characterized by highly variable mineralogical, physical, and mechanical properties. Serpentinites from Moeche (North Western Spain) have been studied to establish their mineralogical, petrographic, and textural characteristics, as well as their physical and mechanical parameters and the factors influencing rock failure, to evaluate the possible use of these rocks either for new construction or for conservation-restoration of the architectonic heritage of the region. In this paper, we highlight the importance of a detailed mineralogical and petrographic characterization in the fracture zones, which will determine the viability of quarrying the stone. A strong correlation between the petrographic features and the uniaxial compression strength values has been observed. The most important aspects were found to be the rock texture, the mineralogical composition of the fracture area and foliation, although mineralogy was also found to be involved (% of carbonates) in the strength of the stone. An important preliminary result of the study was the low asbestos content of these serpentinites, which will help in the potential re-opening of the quarries.

Keywords: serpentinites; rocks characterization; dimension stone; architectural heritage

1. Introduction

Serpentinites are metamorphic rocks formed from the alteration of ultramafic rocks. These alteration processes lead to the hydration of original mineral phases that were formed prior to serpentine and other minerals [1]. Macroscopically, foliation, which bestows a clear anisotropy to these rocks, brecciated areas, and carbonates, filling fractures or replacing serpentine minerals, are quite common features of serpentinites around the world. As a consequence of their mineralogical and structural variability, serpentinites are very heterogeneous rocks. They have been used as construction materials since ancient times; many monuments and historical buildings are made of these important heritage stones [2–4]. Serpentinites appear recurrently in commercial catalogs as green marbles due to the frequent replacement of serpentine minerals for carbonates [5,6]. However, they are not marbles, and a detailed characterization from several points of view (mineralogical, physical and mechanical) is needed if the rocks can be applied either in construction or conservation-restoration of the architectonic heritage.

A few published papers refer to the physical and mechanical properties of serpentinites. Coumantakis [7] observed that in ultramaphic rocks, geomechanical behavior depends on the degree of serpentinization. Other authors [8] report data from two construction projects in which serpentinites are used as construction material: The Hepp damn (Indonesia) and the Berke powerhouse access tunnel (Turkey). Oszoy et al. [9] characterize serpentinites, among other stones, for the Yakakayi dam site (Turkey), highlighting their different behavior depending on the degree of alteration. Marinos et al. [10], who also study serpentinites from the perspective of rock mass, report that the value of the Geological Index Strength (GSI) considerably differs depending on the petrographic and structural variations of serpentinites. The results of these studies have led to a common conclusion: The behavior of serpentinized rock masses depends on the degree of alteration and on the structure or foliation affecting the rock.

Other studies have approached the characterization of serpentinites without taking into account rock mass, but rather focus on the rock as dimension stone, both for conservation-restoration and new building. In this sense, Christensen [11] describes their findings concerning the elastic properties of serpentinites and peridotites obtained from P and S wave velocities. Other authors [12] have studied serpentinites from Egypt used as dimension stones in heritage, and Diamantis et al. [13] have proposed several correlations among the physical and mechanical properties of Greek serpentinites used in heritage. Kurtulus et al. [14] have determined dynamic engineering values, as well as the geotechnical and mechanical properties of serpentinized ultrabasic rocks in NW of Turkey, showing some correlations between different parameters. Navarro et al. [15] studied the serpentinites from Macael (S of Spain) used as dimension stone, obtaining varied results with respect to their mechanical properties, owing to the mineralogical differences between samples. Other authors [16] have compared two serpentinites from the same quarry in Macael (SE of Spain) with different degrees of carbonation. In addition, they remarked on the differences found in the main parameters used in the dimension stone industry among the samples tested. More recently, Navarro et al. [6] have carried out a complete study with six varieties of carbonated and non-carbonated serpentinites from the SE of Spain. They showed how carbonation of serpentinites greatly influences the behavior of these rocks when used as dimension stone. Pereira et al. [5] have remarked on the need for petrographic and mineralogical data in order to be able to decide on the utility of serpentinites as dimension stones.

A significant amount of architectonic heritage found in this part of Galicia was built using this kind of rock, which is known locally as “Pedra de Toelo” [3]. The reason of their extensive use in the past in this area is that this stone presents the quality of being much softer and ductile to the chisel of the stonemason than the granite, another frequently used stone in the area. This characteristic allows a more refined sculpts as well as an easier finishing and polishing. Its crass shine and its color, varying from greenish to dark gray, pinkish and bluish, as well as the presence of abundant veins and a particular mottled, gives a pleasant polychrome appearance acquiring a variable tone with the changes of luminosity, originating several kinds of works. However, all these features trigger a greater degradation of the material over the passage of time [17]. This is why most of the architectural heritage sites built on this stone are in very bad states of conservation at present, and in need of an intense conservation-restoration, including replacement of some blocks. Also for this reason, it is very important to analyze the content of asbestos in these rocks, because a high content of the fibrous minerals should prevent any intention of re-opening the quarries, to obey the very strict European laws (e.g., Directive 2009/148/EC on the protection of workers from the risks related to exposure to asbestos at work).

The quarries in this area were mined for a long period in the past centuries. In fact, they are found in the commercial catalogs under the commercial name of “Verde Pirineos” by Marmolera Gallega, S.L.; currently, a mining company is carrying out new studies and is considering the possibility of resuming mining activity. The name of the company is omitted for confidential reasons.

Preliminary studies on stones from Moeche focused on the mineralogy and the physical and mechanical characteristics of different varieties of serpentinites of the region and their use as a dimension stone in the region, which also forms part of the architectural heritage of the area [3,18–20]. The heterogeneity of serpentinites was made clear, even within a single outcrop. The only geotechnical standard that contemplates the requirements of physical and mechanical behavior for serpentinites as natural stone is the American C1526-02 standard [21]. In this document, the range of accepted values for water absorption (0.2% in exteriors and 0.6% in interiors) and the minimum values for uniaxial compression strength (69 MPa) and bulk density (2560 kg/m³) are specified as the requirements.

The present paper studies the mineralogical, physical, and mechanical properties of one of the main bodies of serpentinites in Spain, located in the area surrounding Moeche (Galicia, NW of Spain). The uniaxial compression strength (UCS), elastic moduli (E_s , ν_s), bulk density (ρ), and water absorption (a) have been determined, as well as the characterization of the mineral composition carried out using X-ray diffraction and the study of thin sections. This work also includes a detailed description of the failure surfaces developed during the UCS tests. Accordingly, ultrasonic wave velocities were measured and the results were compared to bulk density, the UCS, and the elastic moduli in search of connections that could help to explain their behavior. Furthermore, this characterization could also facilitate the commercial use of these stones, both for construction and conservation-restoration purposes.

The objectives of this work are focused on describing the main properties of serpentinites from Moeche and to determine the mechanisms of rock failure to facilitate the evaluation of these serpentinites as potential construction and conservation-restoration material.

2. Geological Context

The study area is located in the NW of Spain and belongs to the Cabo Ortegal Complex, one of the five allochthonous complexes outcropping in the NW of the Iberian Massif and framed within a context of collision between Gondwana and Laurasia [22–25] (Figure 1).

The ultramafic rock outcroppings in this complex are in large part allochthonous units, the stacking of nappes being the consequence of subduction and collision in the early phases of the Variscan orogeny in Northwestern Iberia. The different units are fragments of the lithospheric mantle at the base of the ophiolitic complexes and they have undergone several metamorphic events before being piled up and incorporated into the autochthonous terrane [19]. Serpentinization and tectonic structure is well known [23,24,26,27], and three different units can be distinguished at the complex: The Basal Unit, The Ophiolitic Unit, and the Upper Unit. Within the Ophiolitic Unit, the Somozas Mélange has been described, where two sub-units can be differentiated. The upper sub-unit, 800 m thick, is made up of a highly sheared matrix of serpentinites surrounding tectonic blocks and slices of variable size and continuity, with gabbros, diabbases, granitoids and volcanic rocks, and intercalations of phyllites and phyllonites. In this sub-unit, inclusions of sandstones, conglomerates and marbles can also be found, but are less common. In the case of the lower sub-unit, which can reach a thickness of 1000 m, is a *mélange* with a matrix of ocher-colored or blue phyllites [24]. Our samples were collected in quarries located in Moeche, in one of the massifs from the uppermost unit of this complex.

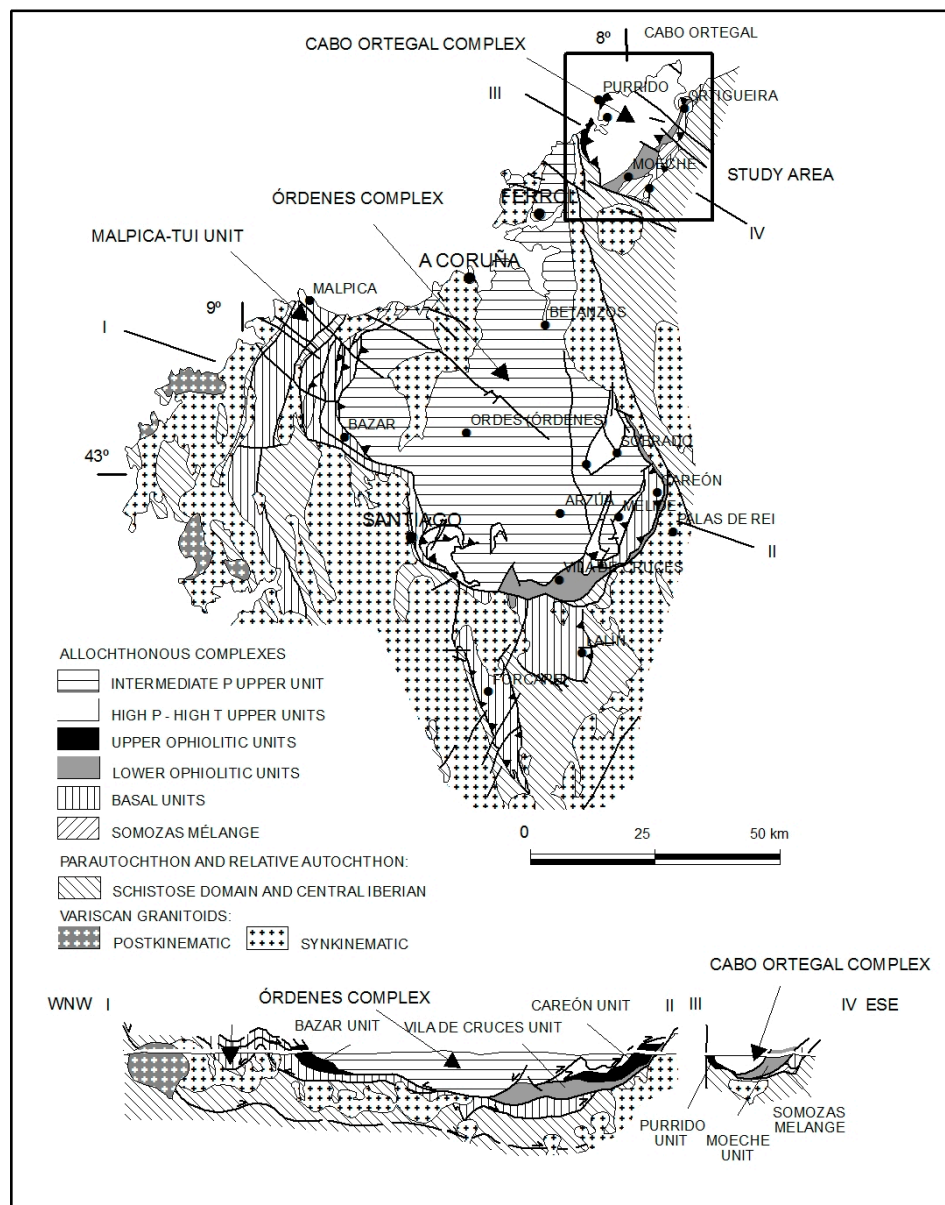


Figure 1. Geological map of the area according to Albert et al. [25]. The solid black arrow shows the Moeche study area.

3. Materials and Methods

3.1. Sampling

Seven block samples were collected from abandoned quarries close to the village of Moeche (Figure 2a), measuring approximately $30 \times 30 \times 20$ cm (Figure 2b). The quarries are located in Monte Ferrerías (samples from blocks 2, 3, 4, 5, 7, 8), and Monte Gradoy (samples from block 10). The samples were collected directly from the outcrops and also from abandoned blocks from previous quarry stonework. Although the structure of these stones is very chaotic, with heterogeneous presence of foliation, fractures, etc. . . , the general direction of the quarry beds follows the principal direction of the regional structure.

A laboratory core drill and cutting machines were used to prepare cylindrical specimens, with diameters between 50.7 and 51.1 mm and lengths between 101 and 104 mm. Thus, the length-to-diameter ratio was 2.0, in accordance with the accepted suggestions for uniaxial compression tests in rocks [28].

The samples analyzed and the tests carried out are shown in Table 1.

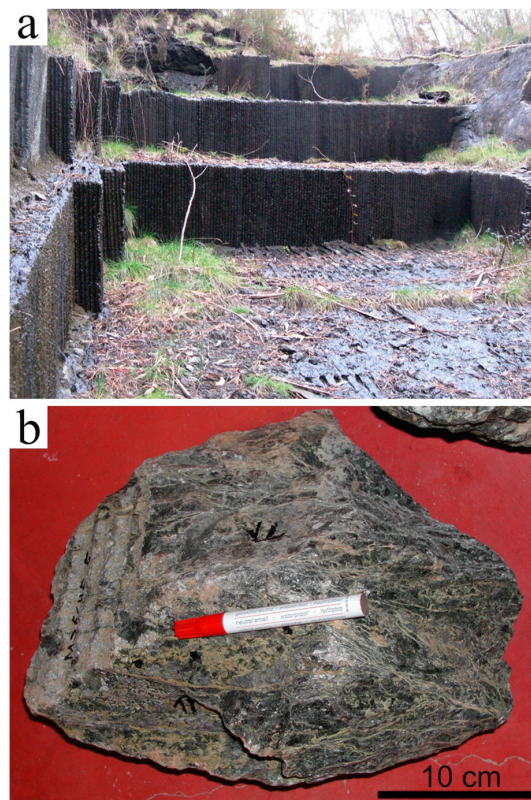


Figure 2. (a) Abandoned quarry in Monte Ferrerías (Moeche) where sampling was carried out. The high of quarry beds is around 1 m; (b) serpentinite block sample from the same quarry.

Table 1. Samples used in this study and the tests and analyses carried out. In the Petrography column, the number of thin sections prepared is indicated in parentheses. The last row shows the total number of samples, tests, and analyses performed. (Id): Sample identification; (UCS): Uniaxial compression strength test; (V_P/V_S), the ratio between P-wave and S-wave velocities.

Id	Bulk Density	Petrography	UCS	V_P/V_S	Strain Gauge	XRD	Water Absorption
M-2d	X	X (2)	X	X	X	X	-
M-3a	X	X (1)	X	X	X	X	-
M-3b	X	X (1)	X	X	X fail	X	-
M-3c	X	-	-	X	-	X	X
M-3e	X	X (1)	X	X	X	-	X
M-4a	X	X (1)	X	X	X fail	X	-
M-4c	X	X (1)	X	X	X	X	-
M-5a	X	X (1)	X	X	X	X	-
M-5b	X	X (1)	X	X	X	X	-
M-5c	X	X (1)	X	X	X	-	X
M-7a1	X	X (1)	X	X	X	X	-
M-7a2	X	-	-	X	-	-	-
M-7b1	X	-	-	X	-	-	-
M-7b2	X	X (1)	X	X	X	X	X
M-7c1	X	-	-	X	-	X	X
M-7c2	X	X (1)	X	X	X	-	X
M-8a	X	-	-	X	-	X	-
M-8c	X	X (1)	X	X	X	X	-
M-8d	X	X (1)	X	X	X	X	X
M-10a	X	X (2)	X	X	X	X	-
M-10b	X	-	-	X	-	X	X
Total	21	17	15	21	15	16	8

The working hypothesis was that the serpentinites would fail across bands or discontinuous zones where highly variable mineralogy might appear, and mechanical tests have proved this to be true in most cases.

Some extra samples were analyzed to describe the possible content of asbestos in these rocks.

3.2. Physical Properties

Bulk densities were obtained for each cylindrical sample, and geometrical volume was determined. Thus, in each specimen, the average diameters (D) from six measurements were recorded (two at the upper end, two in the middle, and another two at the lower end, and the average height (H) from three measurements taken along the probe axis and equally spaced at approximately 120°). Specimen weights were determined using a scale after oven drying to constant mass.

Water absorption (a, measured as %), the ratio between the water mass in a saturated sample and its dried mass, were determined after the samples had been subjected to 48 h of immersion in water, after which they were weighed on a precision balance. Dry mass measurements were taken after oven drying at 60 °C until constant mass, using some of them to test the water absorption.

ASTM C-1526-02 was followed to test properties such as water absorption (a) or bulk density (ρ) [20].

3.3. Ultrasonic Test

The study of sound waves was performed at the Laboratory of Applied Petrology of the CSIC-University of Alicante Associated Unit, following the ASTM C1721-15 standard. This involved the coupling of two piezoelectric sensors on opposite faces of the sample. A viscoelastic gel was used to achieve a good connection between the sample and the transducers. The travel time was registered using Panametric non-polarized transducers (1 MHz) connected to an oscilloscope to detect and identify the wavefronts. The length and travel time in each sample allowed the wave propagation velocities (V_P and V_S) to be calculated.

Specimens of 50 mm diameter and 100 mm length were tested after being oven dried and subsequently cooled in a desiccator. The same specimens were later used to perform the uniaxial compression tests. Nine samples were also tested after they had been soaked in water for 48 h.

Elastic dynamic moduli were obtained indirectly from the ultrasonic tests [29] using the following expressions:

$$\nu_d = \frac{\left(\frac{V_P}{V_S}\right)^2 - 2}{2 \cdot \left[\left(\frac{V_P}{V_S}\right)^2 - 1\right]} \quad (1)$$

$$E_d = 2 \cdot \rho \cdot V_S^2 \cdot (1 + \nu_d) \quad (2)$$

ν_d : Dynamic Poisson coefficient.

V_P : Compressional ultrasonic wave velocity

V_S : Shear ultrasonic wave velocity

E_d : Dynamic Young modulus

ρ : Bulk density

3.4. Uniaxial Compression Strength and Elastic Modulus (Static)

Uniaxial compression tests were carried out with the same specimens used for the ultrasonic tests. The load rate applied was 0.1 MPa/s, and failure was reached after 11.3 min (average value).

Simultaneously, the elastic parameters E_s and ν_s —the static Young modulus and the Poisson coefficient—were measured with the help of two pairs of electrical strain gauges (for axial and diametric strain) appended to the middle portion of the curved surface of the specimens with epoxy resin adhesive after cleaning the surface with acetone and polishing to get a homogeneous surface. The Young

modulus was obtained as the average slope of the straight portion of the stress-strain curve, one of the three methods included in the standard EN 22-950-90/3 [30].

3.5. Mineralogy and Petrographic Analyses

The mineralogical composition was determined by X-ray powder diffraction analysis (Bruker D8 Advance) of bulk rock with Cu K α radiation and a velocity of 2 θ /min. The semiquantitative determination of the different proportion of the detected phases was done following Rietveld's method [31]. The equipment used is a Siemens D-500 (40 KV and 30mA) diffractometer using CuK α radiation ($\lambda = 1.5437\text{\AA}$) Ni-filter, equipped with the Diffract ATV3 software package, at the University of Salamanca.

The petrographic study was carried out on thin sections from the fractured area after testing samples for compression strength. Careful reconstruction using adhesive tape was required for each broken sample. Then, thin sections perpendicular to the specimen axis were obtained after embedding the specimen in resin to regain a single unit. Samples M-2d and M-10a were also cut parallel to the axis. A complete petrographic examination was done following Reference [32] to describe the mineralogy and textures as recommended by Reference [33]. A Leica DM2500P microscope under transmitted light was used for this purpose.

Selected samples were also studied through Scanning Electron Microscopy (SEM) in order to detect a suspicious content of fibrous minerals, which would immediately suggest avoiding any further quarrying. For SEM, samples were prepared in aqueous suspension in an ultrasonic bath, and SEM was recorded with a Zeiss EM 900 instrument.

4. Results

The results obtained for the physical and mechanical properties are summarized in Table 2.

Table 2. Statistical results of the mechanical properties evaluated. (CV), coefficient of variation (CV is the ratio of the standard deviation to the mean; (ρ), bulk density, (a), water absorption; (V_P), P-wave velocity; (V_S), S-wave velocity; (V_P SAT), P-wave velocity in saturated samples; (V_S SAT), S-wave velocity in saturated samples; (E_d), dynamic elastic modulus; (UCS), uniaxial compression strength; (E_s), static elastic modulus.

Statistic Parameter	Max	Min	Average	Median	Standard Deviation	CV	Total Number of Measurements
ρ (kg/m ³)	2838	2597	2747	2759	75	3%	21
a (%)	0.7	0.1	0.4	0.5	0.2	50%	8
V_P (m/s)	5914	1859	4673	4731	1098	23%	21
V_S (m/s)	3342	1264	2657	2722	567	21%	21
V_P/V_S	2.05	1.35	1.75	1.23	0.18	10%	21
V_P (m/s)(Sat)	5983	3258	5079	5082	837	16%	9
V_S (m/s)(Sat)	3257	1608	2738	2728	499	18%	9
E_d (GPa)	78	9	51	49	20	39%	21
Poisson (ν_d)	0.34	0.07	0.25	0.25	0.07	28%	20
UCS (MPa)	119.6	24.2	57.1	59	24	42%	15
E_s (GPa)	66	12	39	44	16	41%	15
Poisson (ν_s)	0.48	0.08	0.22	0.18	0.14	64%	13

Concerning the physical properties, the average bulk density was 2747 kg/m³. The highest values found corresponded to the highest values determined for V_P , which were associated with sample M-7b2. The water absorption value was 0.4%, ranging between 0.1%–0.7%. One of the lowest values obtained also had a low bulk density and the lowest V_P (sample M-10b), although there were no significant differences with respect to the other samples.

With regard to the mechanical properties, the uniaxial compression strengths (UCS) values were highly discordant, where the lowest value was observed for sample M-5c (24.2 MPa) and the highest

for sample M-2d (119.6 MPa). The average value for the fifteen specimens tested was 57.1 MPa, the coefficient of variation, defined as the ratio of the standard deviation to the mean, being especially significant and reaching 41%. This reflects the enormous variation in the values obtained for this parameter, and the lack of meaning of averages in this context (Table 2). Sample breakdown was reached after an axial strain between 0.07%–38% (mean 0.20%), and the E_s from 12 (specimen M-10a) to 66 GPa (specimen M-7b2), with a mean of 39 GPa. Additionally, values ranged from 0.08–0.48 for the Poisson ratio, with a mean of 0.22. Most of the breakdown occurred following previous discontinuity surfaces, frequently with light colors in hand sample. The angle between the perpendicular line to the failure surface and the axis of the specimen varied between 60° and 70°.

This scattered behavior occurs quite frequently and is well known in foliated rocks [34–36] as its strength is a function of the angle between the loading axis and the orientation of anisotropy planes (β). The strength is at its maximum when β is equal to 90° and at its minimum when the β angle is around 30° ($45^\circ - \varphi/2$, being φ the friction angle of discontinuity in the Mohr-Coulomb breakdown criterion). Taking this into account, it is possible to evaluate rock anisotropy using the anisotropy ratio [37,38], defined as the ratio of compressive strength at $\beta = 90^\circ$ and the minimum strength observed ($\sigma_{c90}/\sigma_{cmin}$). The maximum UCS obtained in the Moeche serpentinites was 119.6 MP (sample M-2d) in a nodulous serpentine with scarce planes of foliation normal to the direction of the load ($\beta = 90^\circ$). A foliated serpentinite, on the other hand, with $\beta = 30^\circ$ and a fracture surface in a talc rich area, showed the minimum UCS (24.2 MPa, sample M-3b). This sample would be classified as high anisotropy since the ratio $\sigma_{c90}/\sigma_{cmin}$ is between 4 and 6. Other samples with similar foliation orientations ($\beta \approx 30^\circ$) show a lower anisotropy ratio, which highlights that the mechanism involved in the failures also depends on the intensity of foliation, the amount of nodulous areas, and the mineralogical composition of the failure planes. Even still, the typical behavior of a foliated rock is clearly present.

According to the Reference [39] classification for the uniaxial compression strength in rocks (Figure 3), the samples were classified in groups that included weak to very strong rocks, with most of the samples being classified as strong (50–100 MPa). In most cases, the relative E_s/UCS ratio [40] was medium, although occasionally the ratios were high.

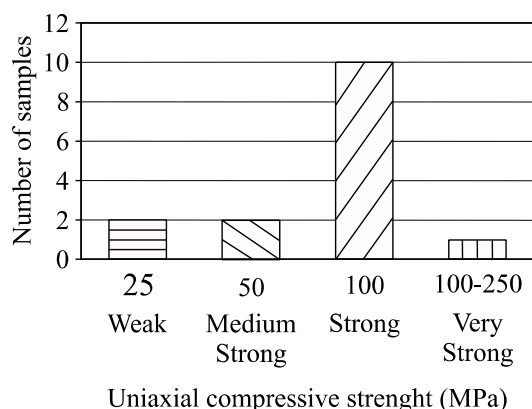


Figure 3. Samples from Moeche grouped according to their UCS based on the ISRM classification system [39]: Weak (UCS > 25 MPa), medium-strong (25–50 MPa), strong (50–100 MPa), and very strong (>100 MPa).

As for the ultrasonic velocities, V_P ranged from a low of 1859 to a maximum of 5914 m/s in dried specimens. The average was 4673 m/s and the relation between the standard deviation and the average was 23%. In the case of saturated samples, the mean V_P was slightly higher, 5079 m/s. The V_S in dry specimens was between 1264–3342 m/s, with an average of 2627 m/s and a coefficient of variation of 21%. Under wet conditions, the average was also slightly higher: 2738 m/s. The V_P/V_S ratio ranged between 1.35–2.05, with a mean of 1.75.

Samples M-10a and M-10b had the lowest V_P under dried conditions, obtaining values below the average, with less than 2000 m/s. Samples M-7, M-5, and M-2d displayed the highest V_P values, all of them above 5000 m/s. We continue to study the correlation between ultrasonic velocities and the other parameters to understand the results, but the preliminary explanation seems to be related to the different mineralogical composition of samples, from only serpentine (antigorite) to a mixture with talc and carbonates.

The dynamic elastic modulus ranged between a minimum of 9 GPa and a maximum of 78 GPa, with a mean of 49 GPa. Evidently, the highest and the lowest values were associated with the samples with the maximum and minimum V_P values.

With respect to mineralogy, the results of the x-ray diffraction (XRD) (Table 3) showed that serpentine polymorphs (antigorite, lizardite, and traces of chrysotile) were the main minerals in all of the samples, followed by magnesite, whereas talc and dolomite appeared in smaller proportions. The latter was detected in only four samples, but these data are very important in terms of conservation-restoration, as this carbonated stone, locally called Pedra de Toelo or Pedra de Moeche, was used for the sculptures in façades of many buildings and sculptures of the region [3,17] (Figure 4).

Table 3. Percentage (%) of the phases detected by XRD. Semi-quantitative analysis.

Sample	Serpentine	Magnesite	Talc	Dolomite
M-10a	100	0	0	0
M-2d	89	0	0	11
M-8c	84	12	4	0
M-4c	79	17	4	0
M-7c2	79	14	7	0
M-4a	78	16	6	0
M-7b2	71	23	6	0
M-8d	68	25	6	0
M-7a1	62	29	9	0
M-5a	53	38	9	0
M-3e	50	34	12	3
M-5b	50	24	25	0
M-5c	50	24	25	0
M-3b	49	41	8	2
M-3a	48	40	10	3
Max	100	41	25	11
Min	48	0	0	0
Average	67	22	9	1
Standard Deviation	16.3	12.4	7.3	2.9

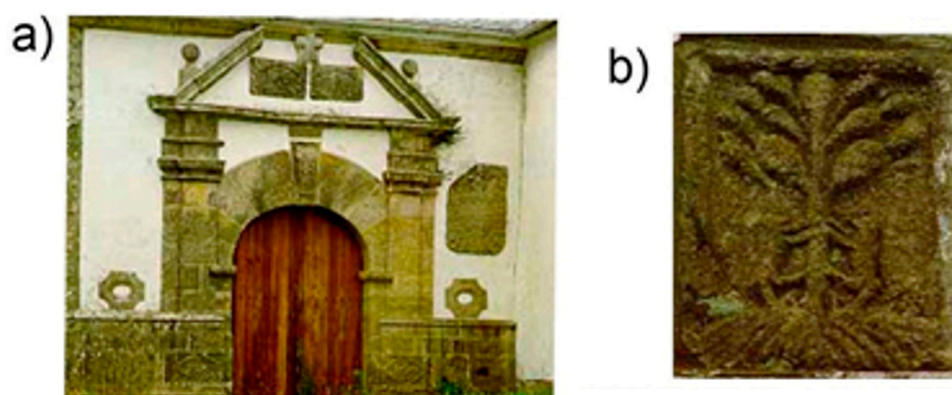


Figure 4. Details of the use of the carbonated serpentinite (Pedra de Toelo or Pedra de Moeche) in the architectural heritage of Galicia. This stone can be found in monuments and historical buildings from the Middle Ages. (a) Door lintels, and other architectonic ornaments in the façade of Labacengos church, in Moeche (16th century); (b) coat of arms of the Monastery of Oseira (oso means bear in Spanish).

Different textures were found in the Moeche serpentinites depending on the original mafic mineral and on the degree of recrystallization. In the thin sections analyzed, it was possible to distinguish the following:

- Preferentially mesh texture and sometimes hour-glass texture. This is a typical texture of olivine serpentinization and is frequently observed in nodulous areas (not affected by foliation or fractures) (Figure 5a).
- Bastite texture. Serpentine mineral aggregates elongated and with similar orientation. This is a serpentine that has replaced old pyroxenes, and in these cases, the presence of oriented magnetite following pyroxene exfoliation surfaces is quite frequent (Figure 5b).
- Thorn texture. This has a higher degree of crystallization than the previous textures and is developed from them. Original minerals may not be clear, although there is a tendency for this texture to appear normal to olivine, and parallel to the pyroxenes (Figure 5c).
- Fibrous serpentine (chrysotile) growing normal or parallel to fractures (Figure 5d).

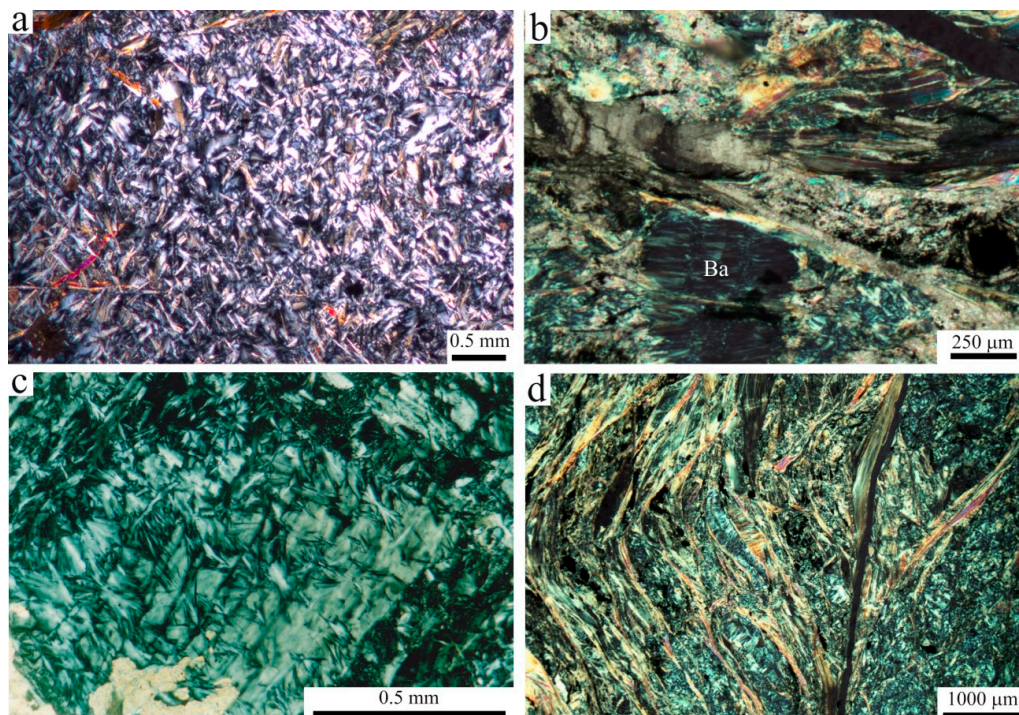


Figure 5. Textures found in the Moeche serpentinites (Crossed Nichols): (a) Mesh texture (M-8c); (b) bastite (Ba) (M-3b); (c) thorn texture beginning to recrystallize on bastite (M-2d); (d) fibrous serpentine (possibly chrysotile) (M-10a).

In addition, most of the samples included chromite spinels and chromites as accessory minerals, whose borders are frequently replaced by magnetite.

The Moeche serpentinites usually showed an irregular foliation with varying directions, and wavy surfaces marked by veins filled either with carbonates or by slices parallel to them, where talc and/or serpentine was predominant. Frequent fractures running in all directions and filled with carbonates were also observed.

Foliation and fractures often affected the whole rock, but sometimes they were less persistent, leaving nodular areas with no discontinuities. These areas were of a dark green color in the hand specimens and under the petrographic microscope, serpentine, talc and carbonate could be distinguished. Some textures were the remains of the original mineralogy (olivine and pyroxene) (Figures 6 and 7).

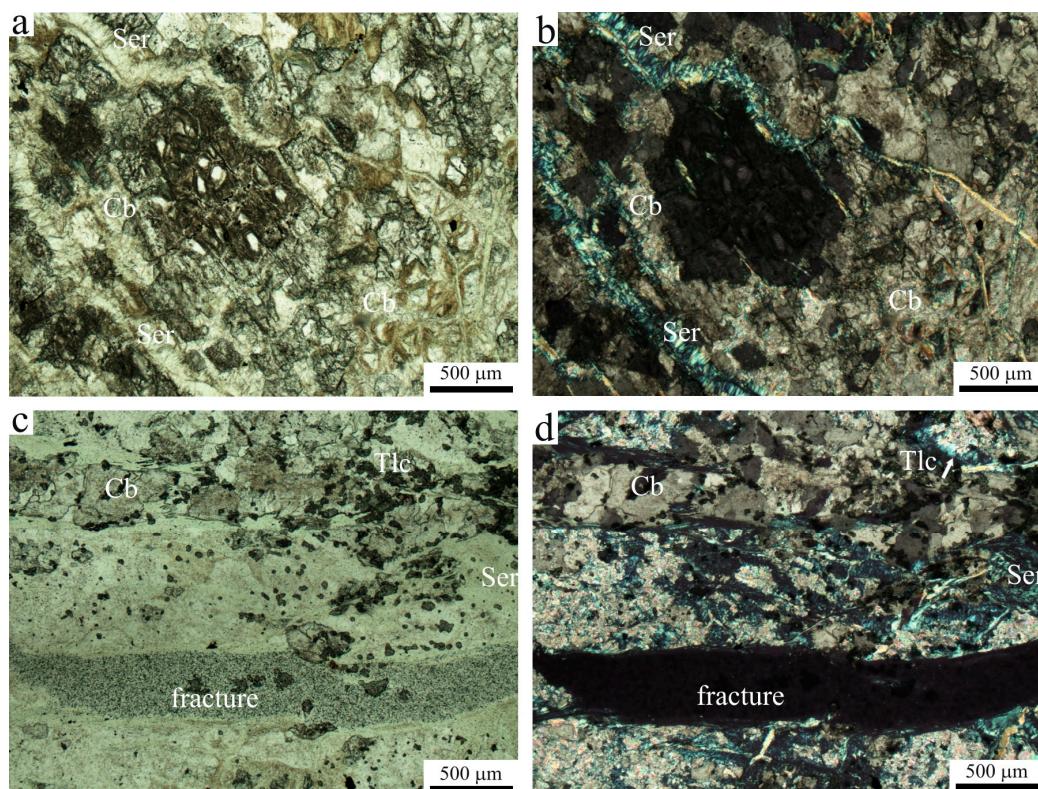


Figure 6. (a,b) Sample M-4a. Carbonation of olivine in an early stage of serpentinization with serpentine with mesh texture (a, Parallel Nichols and b, Crossed Nichols); (c,d) sample M-3a showing clean carbonates filling fractures, fracture with predominant talc and carbonate crystals aligned following the foliation and parallel to the fracture (c, Parallel Nichols and d, Crossed Nichols). Ser: Serpentine; Cb: Carbonates; Tlc: Talc.

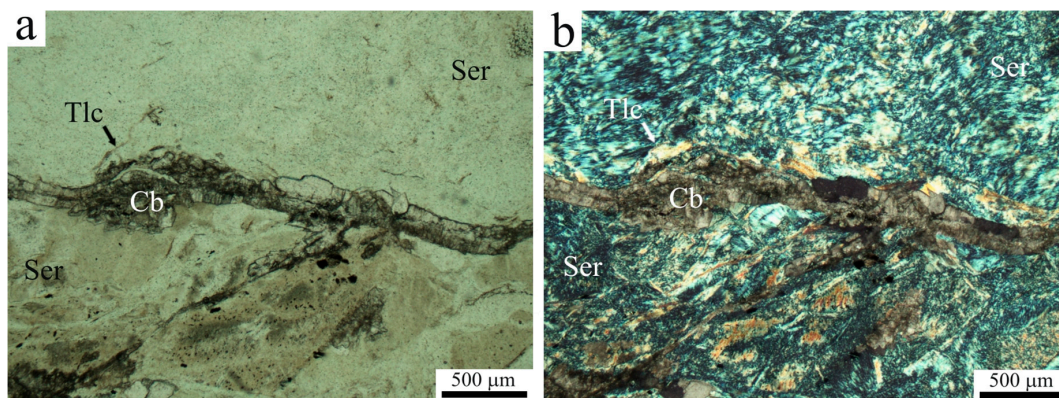


Figure 7. The microscopic aspect of a nodulous sample, not foliated, with serpentine minerals, talc and carbonates, the latter filling a fracture. (a) Parallel Nichols and (b) Crossed Nichols. Sample M-2d. Ser: Serpentine; Cb: Carbonates; Tlc: Talc.

In cases where a relation between rock failure and the mineralogy was established in the uniaxial compression strength test, it was observed that most of the fractures occurred following foliation or in bands parallel to this foliation. In the latter case, the predominant mineralogy was talc, a talc-serpentine association and, occasionally, carbonates filling these discontinuities. In general, the failures were not brittle, except in the case of the nodular samples, in which the fracture surface developed more irregularly and encircled porphyroblasts.

Weak specimens failed following the foliation planes defined by talc (Figure 8a–c) or chrysotile (Figure 8d–f), with an irregular morphology that sometimes seemed to avoid carbonated areas. This is an indication of the higher resistance present in these areas.

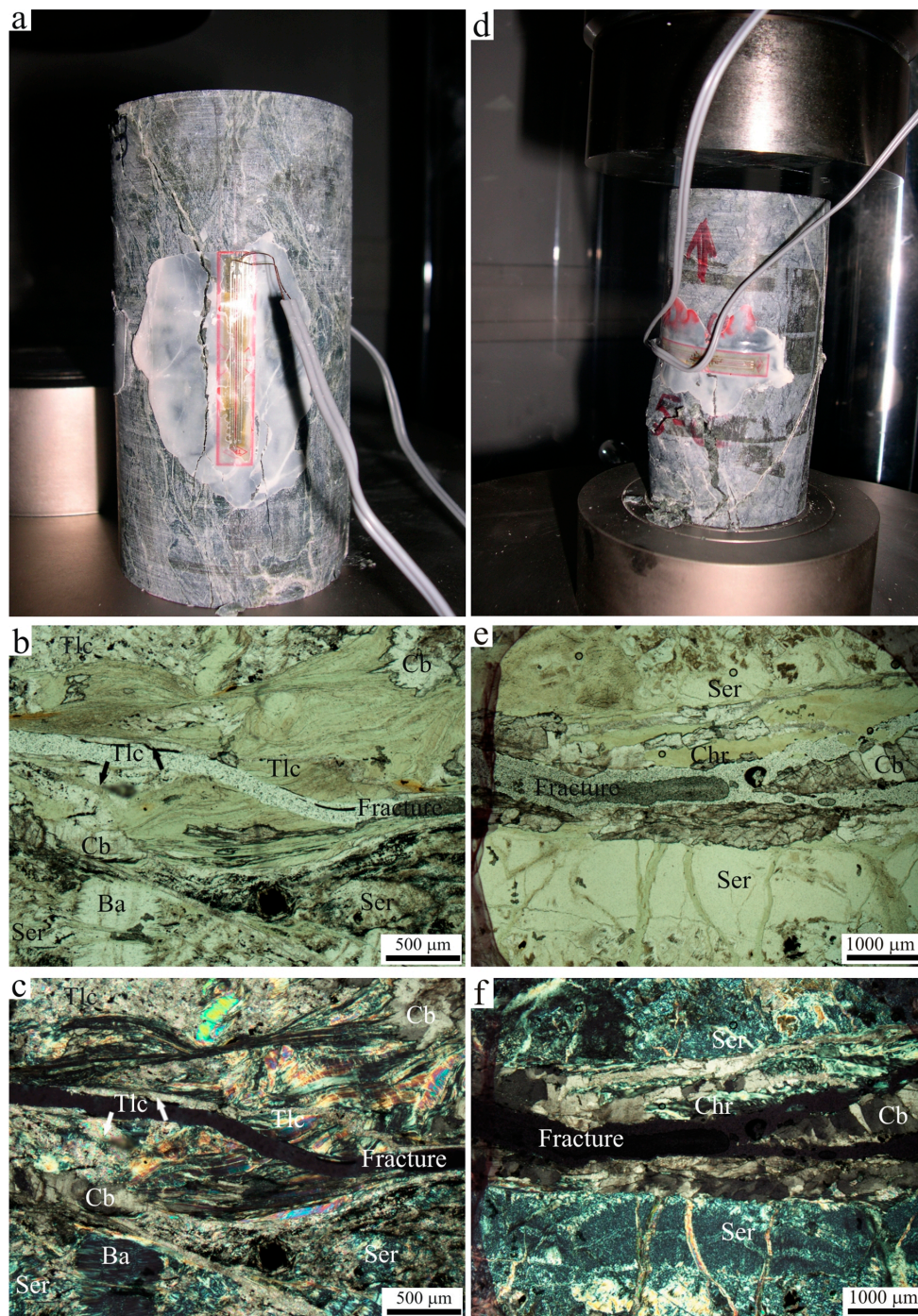


Figure 8. Fractured weak rock samples. Left (a–c): Sample M-3b (UCS = 24 MPa), with the failure surface following foliation with abundant talc in the surrounding areas. Apparently, the fracture does not pass through the most carbonated zones. (a) Sample after UCS testing; (b) Parallel Nichols, and (c) Crossed Nichols. Right (d–f): Sample M-5c (UCS = 25 MPa), with the failure surface following an undulated foliation defined by chrysotile and replacement carbonate in relict olivine where serpentinization has taken place. (d) Sample after UCS testing, (e) Parallel Nichols, and (f) Crossed Nichols. Ser: Serpentine; Cb: Carbonates; Tlc: Talc; Chr: Chrysotile.

In moderately strong samples, the foliation was not as penetrating as in the weak samples, but was more regular (Figure 9a–c). Unlike the weak specimens, the fractures sometimes passed through areas where carbonate recrystallization had occurred (Figure 9d–f).

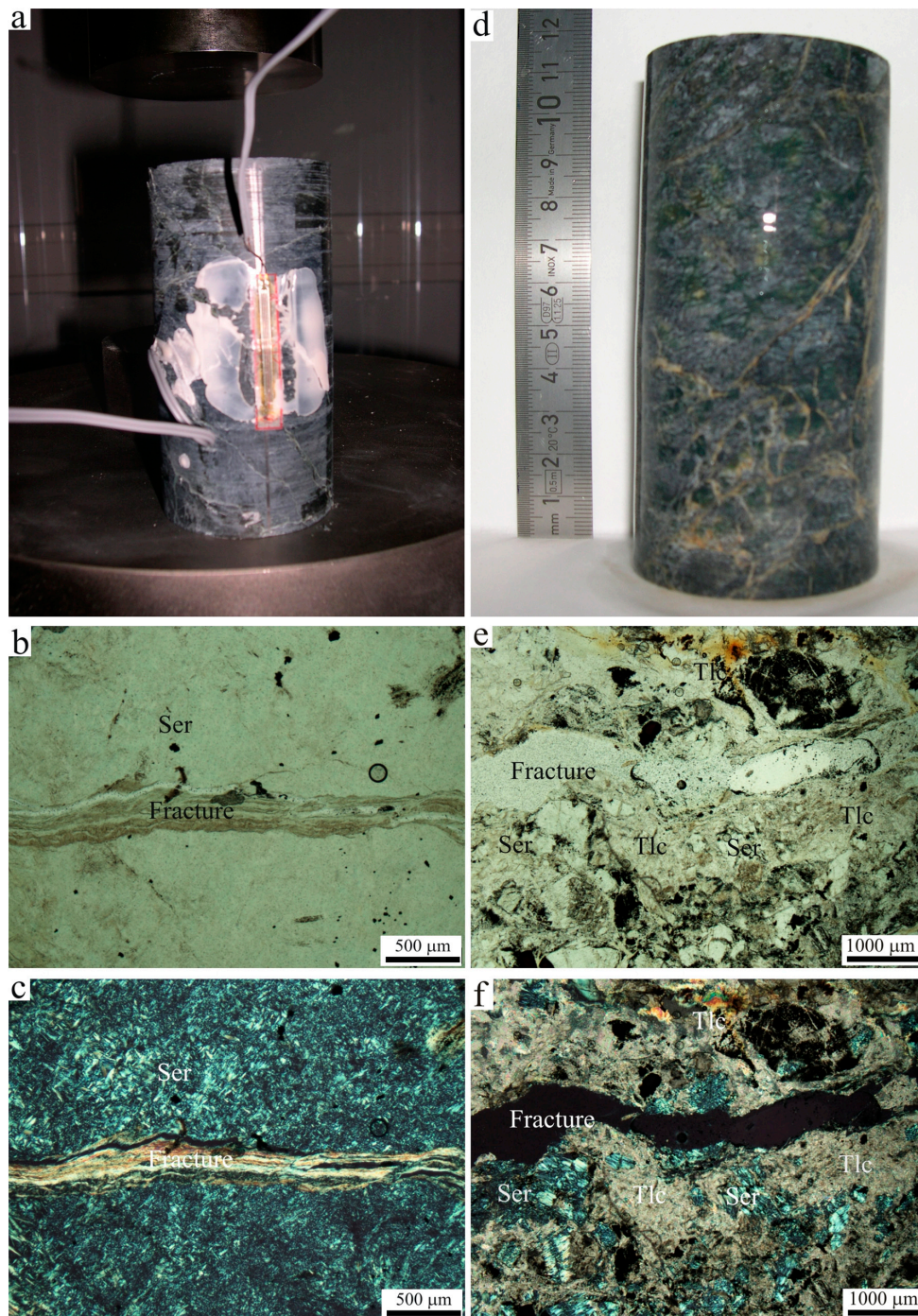


Figure 9. Fractured medium-strong rock samples. Left (a–c): Sample M-10a (UCS = 35.1 MPa) with the failure following the serpentinite foliation in a specimen with few previous fractures. (a) Sample after UCS testing; (b) Parallel Nichols, and (c) Crossed Nichols. Right (d–f): Sample M-8d (UCS = 35.8 MPa) with the fracture following the foliation, defined by intense carbonation and relevant talc contents; (d) Sample before testing; (e) Parallel Nichols, and (f) Crossed Nichols. Ser: Serpentine; Tlc: Talc.

Strong and very strong samples shared a brecciated aspect, but the size of the rock fragments in the strong samples was smaller (Figure 10a,d). Also, in the strong samples, the fractures developed

on foliation planes, filled with carbonate and talc (Figure 10b,c). Moreover, when these foliation planes were not continuous, the fracture tended to surround areas containing relict porphyroblasts, usually completely serpentinized (Figure 10e,f).

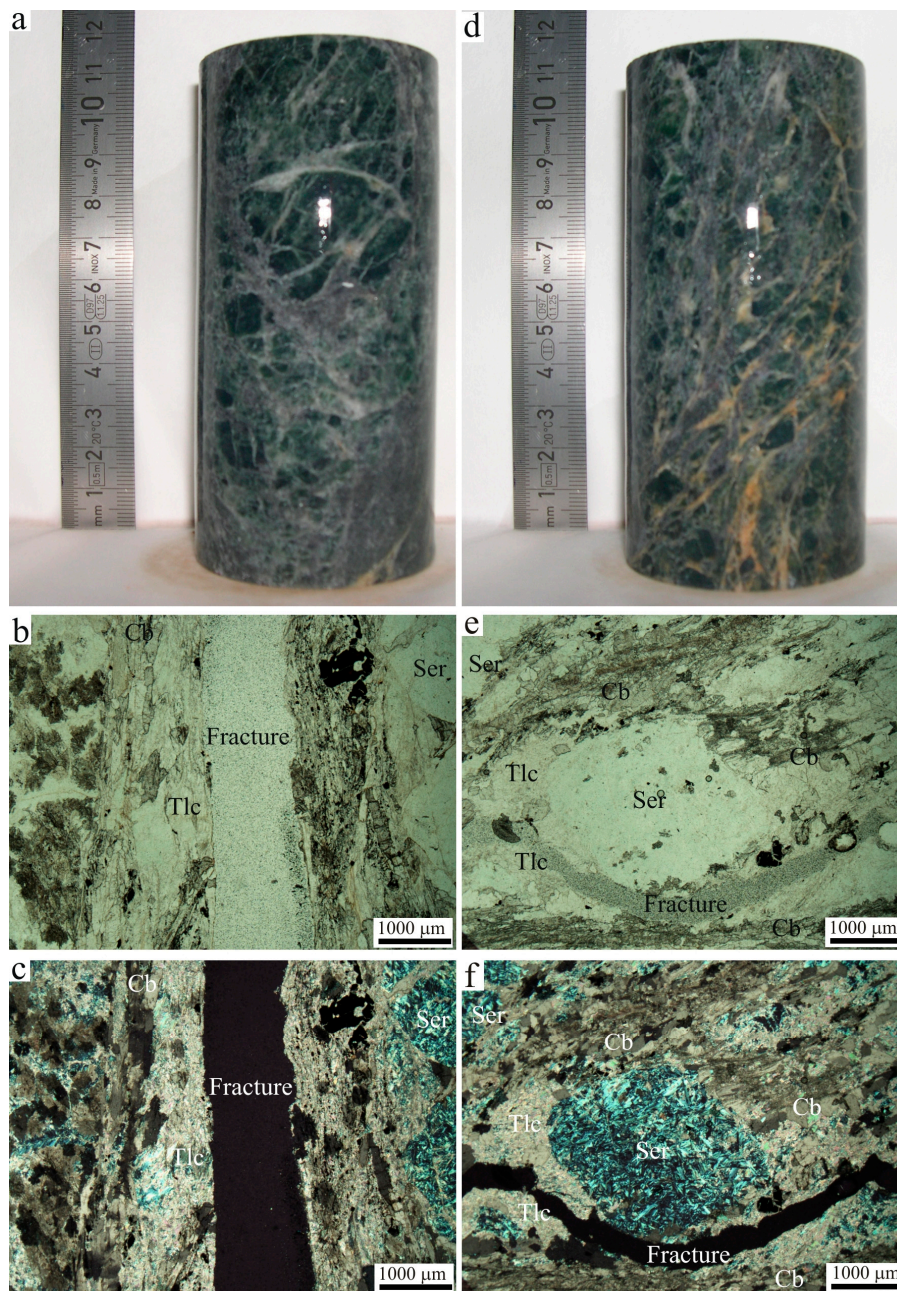


Figure 10. Fractured strong rock. Left (a–c): Sample M-7a1 (UCS = 52.2 MPa) showing the fracture following the foliation defined by talc and carbonates. (a) Sample before testing; (b) Parallel Nichols and (c) Crossed Nichols. Right (d–f): Sample M-7c2 (UCS = 70 MPa), with the failure surface surrounding a serpentinized nodule with talc and carbonates. (d) Sample before testing; (e) Parallel Nichols, and (f) Crossed Nichols. Ser: Serpentine; Cb: Carbonates; Tlc: Talc.

Regarding the very strong samples, their fractures were brittle. It was found that neither the foliation nor the previous fracture orientations were followed, although the latter were clearly visible at the macroscopic scale, but with scarce continuity and irregular orientation (Figure 11).

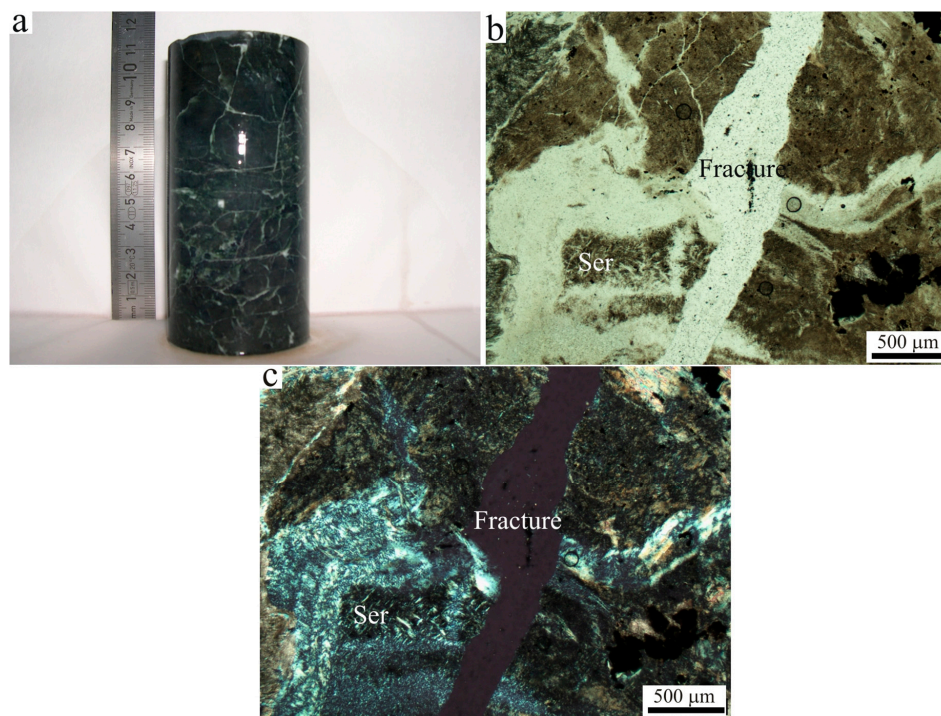


Figure 11. The fractured very strong rock sample. Sample M-2d (UCS = 119.6 MPa). The failure surface does not follow previous discontinuities. (a) Sample before testing, (b) Parallel Nichols, and (c) Crossed Nichols are shown. Ser: Serpentine.

5. Discussion

Moeche serpentinites show a complete transformation of primary minerals in low-grade metamorphism phases, such as minerals from serpentine, carbonate, talc and magnetite, preserving the remains of the chromium rich original spinel [41]. All of these changes cause the mechanical properties of the rock to change, as reflected in the highly variable results obtained during the uniaxial compression strength testing carried out in this study. This parameter is significant for the determination of the behavior of dimension stones, and therefore it is important to establish the factors governing it and other properties, which can be used as an index to predict the uniaxial compression strength of these rocks.

The serpentinites of Moeche generally have low UCS, with an average value of 57 MPa, which is even below the minimum threshold required by ASTM C-1526-02 for susceptible serpentinites to be used as ornamental stones [21]. The maximum water absorption value obtained, 0.7%, is also outside the limit values of the above standard for both outdoor (0.2%) and indoor (0.6%) use. The only ASTM requirement that these rocks accomplish is the minimum bulk density, which was 2600 kg/m^3 , above the minimum value required of 2560 kg/m^3 .

Table 4 compares the properties of serpentinites from different countries reported in the literature and the ones studied here. From this data it can be observed that only the carbonated serpentinites from Macael (SE of Spain) studied by Navarro et al. [6] fulfill all of the requirements set out by the ASTM standard (UCS > 69 MPa; $\rho > 2560 \text{ kg/m}^3$ a < 0.2% (exterior) and a < 0.6% (interior)).

The UCS values obtained are similar to the serpentinites studied in Diamantis et al. [13] and in Kurtulus et al. [14] from the ophiolite complex in Mount Kallidromo, in central Greece and from NW Turkey, respectively. However, differences can be found with respect to the serpentinites from Granada and Macael (SE of Spain) that have an average UCS above 227 MPa. Serpentinites can also have very high values, such as 346 MPa, as is the case of serpentinites from Granada [6] and Egypt [12]. But it is important to highlight that the UCS values obtained in a laboratory setting are highly dependent on multiple factors. Some of these factors are intrinsic (mineralogy, fabric or discontinuities), but others are extrinsic such as shape, size, the relation between width and length and the speed and the direction of the application of

the load [42,43]. UCS values obtained with different protocols (e.g., EN, ASTM) vary even with the same stone, therefore, the comparison between different stones must be approached carefully [44]. The low resistance and significant dispersion found for this property could be explained by the macrostructure of foliated rocks such as serpentinites. The UCS in these rocks depends largely on the relative orientation between the microstructure and the axial load, and therefore the range of dispersion obtained is usually broad [40]. This circumstance often leads to a misinterpretation of the shear strength values of discontinuity planes, where they are thought to correspond to failures in the rock matrix [10]. There are important implications when the global behavior of serpentinitized rock masses is analyzed. Upon studying several outcrops, the same authors proposed a serpentinite matrix uniaxial compression strength of around 40 MPa, which is slightly lower than the average obtained in this study (57 MPa). However, on measuring and comparing the inclinations of the principal planes of the macroscopic Moeche foliation samples tested, it was found that apparently not only the relative orientation between the load applied and the foliation control the uniaxial compression strength of these rocks (Table 5), since there are very weak samples that, macroscopically, are not foliated, such as sample M-3b. This apparently contradicts our hypothesis, but this is in fact not the case, because under the petrographic microscope a microscopic foliation can be distinguished. Therefore, macroscopic observations alone can lead to incorrect conclusions being drawn in cases where apparently foliated specimens are analyzed, as previously noted in Hawkins et al. [28] and references therein. By contrast, the Moeche sample M-2d is weakly foliated at both microscopic and macroscopic scale and its UCS scored the highest of all the specimens tested: 120 MPa. Therefore, as a first conclusion, it can be inferred that foliated samples are weaker than unfoliated ones. In unfoliated samples, although they are sometimes highly fractured, the presence of minerals in the fracture filling—typically carbonates—could hamper the progression of failed surfaces, resulting in a higher UCS.

Table 4. Parameters of different serpentinites compared with the Moeche serpentinites. (m) minimum; (Av) average; (M) maximum; (SD) standard deviation.

Origin		PARAMETER					
		UCS (MPa)	ρ (kg/m ³)	a (%)	V _P (m/s)	V _S (m/s)	
Moeche (Spain) (this paper)	m	24	2600	0.10	1859	1264	
	Av	57	2750	0.40	4673	2657	
	M	129	2840	0.70	5914	3342	
	SD	24	70	0.20	1098	567	
Egypt [12]	m	89	2480	0.01	-	-	
	Av	152	2520	0.10	-	-	
	M	189	2590	0.20	-	-	
	SD	32	30	0.06	-	-	
Greece [13]	m	19	2490	0.14	4842	2425	
	Av	60	2610	0.57	5344	2783	
	M	126	2730	1.84	5789	3109	
	SD	27	60	0	225	170	
Turkey [14]	m	22	2430	0.16	4265	-	
	Av	54	2564	0.46	5018	-	
	M	77	2660	1.33	5461	-	
	SD	16	58	0.39	341	-	
Granada	m	331	2658	0.19	5532	-	
	Av	346	2662	0.26	5646	-	
	M	361	2666	0.33	5589	-	
	SD	51	18	0.10	457	-	
South of Spain [6]	Macael (Carbonated)	m	139	2704	0.10	6024	-
		Av	227	2796	0.13	6078	-
		M	315	2888	0.16	6132	-
		SD	43	32	0.03	309	-
Macael (Non-carbonated)	m	246	2650	0.42	5308	-	
	Av	279	2949	0.48	5203	-	
	M	263	2800	0.53	5378	-	
	SD	61	134	0.10	673	-	

Table 5. Comparative data on uniaxial compression strength obtained for each sample, ISRM classification, macroscopic features, and main general aspects, singularities of fracture and failure angle. Foliation and angle of failure measured from the base of the specimen and typology of the failure surface. ISRM Classification: (W) Weak, (M) Medium-Strong, (S) Strong, (VS) Very Strong.

SAMPLE	UCS (MPa)	ISRM CLASSIF	FOLIATION	MACROSCOPIC FEATURES	FRACTURE SURFACE	FAILURE ANGLE
M-2d	120	VS	No foliation	Nodulous, scarce foliation. Anisotropy due to fractures. Brecciated aspect.	Does not follow previous orientations. Breaks minerals.	30°
M-3a	51	S	60–90°	Foliated, nodulous aspect locally. Anisotropic aspect.	Following foliation, within an area where talc is predominant and aligned carbonates appear.	75°
M-3b	24	W	60–90°	Foliated, nodulous aspect locally. Anisotropic aspect.	Foliation in talc-rich area.	75°
M-3e	52	S	50–60°	Foliated, nodulous aspect locally.	Following foliation.	90°
M-4a	60	S	70°	Nodulous and irregular fractures. Scarce foliation. Anisotropic aspect.	Following fractures.	70°
M-4c	60	S	20–45°	Nodulous and irregular fractures. Scarce foliation. Anisotropic aspect.	Subvertical, locally following foliation.	80°
M-5a	68	S	80°	Irregular. Anisotropic aspect.	Affects both foliated and unfoliated areas.	60°
M-5b	60	S	60–70°	Two main foliations easily recognized in the specimen. Important failure at 60°. Anisotropic aspect.	Previous carbonated plane.	60°
M-5c	25	W	60–90°	Nodulous areas with mineral alignments (80°–85°) and variable fissures (60°–90°). Anisotropic aspect.	Previous carbonated plane.	50°
M-7a1	52	S	70°	Foliated, locally nodulous aspect. Brecciated.	Carbonated foliation with talc-rich bands.	70°
M-7b2	87	S	40–80°	Nodulous, scarce foliation. Anisotropy due to fractures. Anisotropic aspect.	Partially follows foliation.	75°
M-7c2	70	S	45–70°	Foliated, locally nodulous aspect. Brecciated aspect.	Talc in the foliation and parallel to carbonated bands.	65°

Table 5. Cont.

SAMPLE	UCS (MPa)	ISRM CLASSIF	FOLIATION	MACROSCOPIC FEATURES	FRACTURE SURFACE	FAILURE ANGLE
M-8c	59	S	40–65°	Foliation marked by fractures and nodulous zones in between. Brecciated and foliated area.	Foliation, but not always.	45°
M-8d	36	M	No foliation	Irregular due to several orientations. Anisotropic aspect.	Foliation	55°
M-10a	35	M	0–50°	Irregular due to several orientations. Massive aspect.	Foliation	40°

In the light of the dominant role of foliation in these rocks, the question arises as to whether it might be possible that mineralogical differences between the samples could account for the wide dispersion of the UCS obtained. Figure 12 shows the mineralogy of each sample, ordered from the highest to the lowest UCS, and no clear relationship can be obtained between the UCS and the percentage of serpentine, talc, dolomite or magnesite.

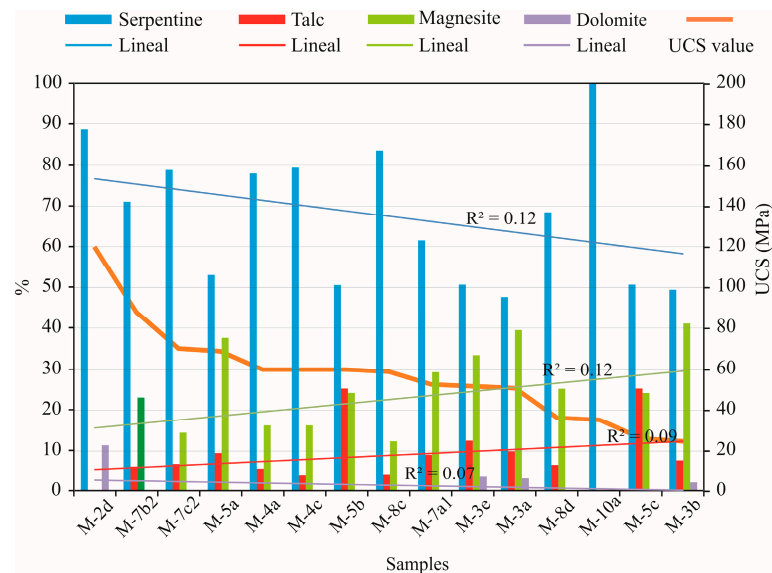


Figure 12. Mineralogy of the Moeche serpentinites according to the semiquantitative results obtained in the XRD analyses. Samples are organized from left to right according to their UCS (MPa). Straight lines represent the linear correlation between each mineral and its UCS.

Nevertheless, the relationship between the percentage of serpentine minerals and the other minerals seems to increase in the strongest samples (Figure 13a), except for sample M-10a, which is comprised of 100% serpentine minerals but has a UCS of 36 MPa. In this sample, the orientation of the load applied and the influence of foliation prevail over mineralogy. Some authors [6,12,15,18] have explained that in similar rocks the carbonate content seems to be responsible for the greater UCS. The trajectories of failure planes in weak rocks were analyzed under a petrographic microscope, and it was observed that the fractures did not progress following the path determined by carbonates. In contrast, they progressed through the carbonates in medium-strong and strong rocks (Figure 13b). This can be explained by the alteration processes that accompany carbonation, which sometimes lead to the formation of microfractures due to the loss of material in these areas [2]. This was also observed by Navarro et al. [6]. In the case of carbonated serpentinites from Macael, the UCS value in the less carbonated samples was much higher than the more carbonated serpentinites. They concluded that in the initial phases of carbonation, carbonates act as cement, increasing the strength. As carbonation progresses, the pressure of crystallization produces fractures, causing the stone to become weak.

The serpentinites from Moeche vary from weak, medium strong, strong and very strong rocks, whose behavior cannot be explained only by their mineralogy. In weak samples there exists slight anisotropy defined not only by the existence of discontinuity planes, but also by a very strong preferred orientation associated with mineralogy (mainly talc); medium strong and strong samples are foliated but this feature is less intense than in the weak samples. Finally, the very strong samples display macroscopic discontinuity surfaces, but these are less continuous than in the previous cases. This fact favors a tendency towards isotropic behavior of the rock, observed microscopically in the irregular shape of the fractures formed without following any foliation or preferred mineral alignment. Glawe and Upreti [8] classified serpentinites with discontinuities of little persistence as very strong rocks, and our data from Moeche corroborates their conclusion.

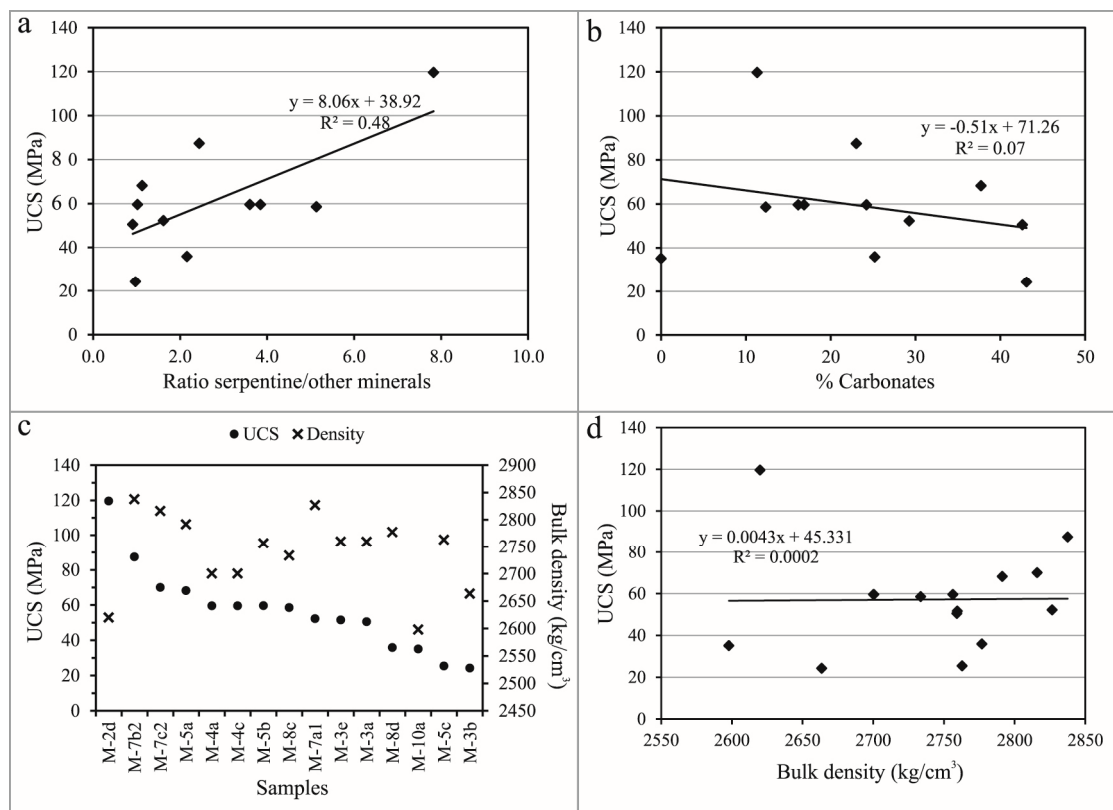


Figure 13. Correlation between UCS and some of the parameters studied: (a) UCS and serpentine/other minerals ratio; (b) UCS and % carbonates; (c) UCS and density bulk for each sample, from the highest value (left) to the lowest (right); (d) UCS test and bulk density.

The enormous difficulties involved in obtaining samples for conducting uniaxial compression tests underscore the need for other types of much simpler tests which may provide relevant information on different mechanical aspects. The correlations between UCS and other tests or analyses are relatively abundant in the literature [45–48], but they do not address serpentinites. One of the most studied correlations is bulk density and the UCS; this correlation is shown in Figure 13c,d for the serpentinites collected from Moeche. The results are not satisfactory at all, showing a very low correlation coefficient (R^2), and disagree with the observations reported by Diamantis et al. [13] for Greek serpentinites, Nespereira et al. [49] for tertiary sandstones, and those of ISRM [39]. Our results are in agreement with the data reported by Reference [50] in sedimentary rock and Reference [51] in basic rocks, where the relationship between the two parameters is very low. Bulk density is directly related to mineralogy, and the fact that they are not well correlated reinforces the idea that the mechanical behavior of serpentinites usually depends on several factors and is much more complex than in other types of rocks.

Other correlations considered in other works are related to the propagation velocities of ultrasonic waves. V_P and V_S correlate well with each other (Figure 14a), but do not correlate well with the mechanical properties obtained from the uniaxial compression tests. It was apparent that the higher the V_P or the V_S , the higher the UCS, but the value of R^2 ranges between 0.17–0.29 (Figure 14b). The same can be said for the correlation between the velocities and bulk density ($R^2 = 0.60$ to 0.59) (Figure 14c) and between the static elastic modulus (E_s) and the velocities (Figure 13d) ($R^2 = 0.74$ to 0.72), in this case using an exponential correlation. An $R^2 = 0.60$ is obtained for E_d and E_s (Figure 14e). Comparing these results with the results for other rocks of different origin, it is common to obtain good correlations between UCS and E_s in granites, basalts and quartzites [52], in sedimentary rocks [46], and even in some serpentinites and peridotites [11]. V_P and UCS are also correlated positively with each other in serpentinites [13,14], but much more pronounced (with R^2 above 0.80 in both cases) than those observed in the Moeche rocks or in the case of serpentinites from Southern Spain, where no

correlation was observed [6]. Finally, Figure 14e also shows the values of E_s and E_d . Their ratio lies between 1 and 2.3, with only two data points below 1. The correlation between both is similar to that obtained by Martínez-Martínez et al. [53] for a wide range of carbonate rocks, and follows the general trend observed by Reference [54]: As the value of E_d increases, so does the E_d/E_s ratio. A good correlation between V_p and E_s was observed by Kurtulus et al. [14], but in this case, the authors observed a linear correlation.

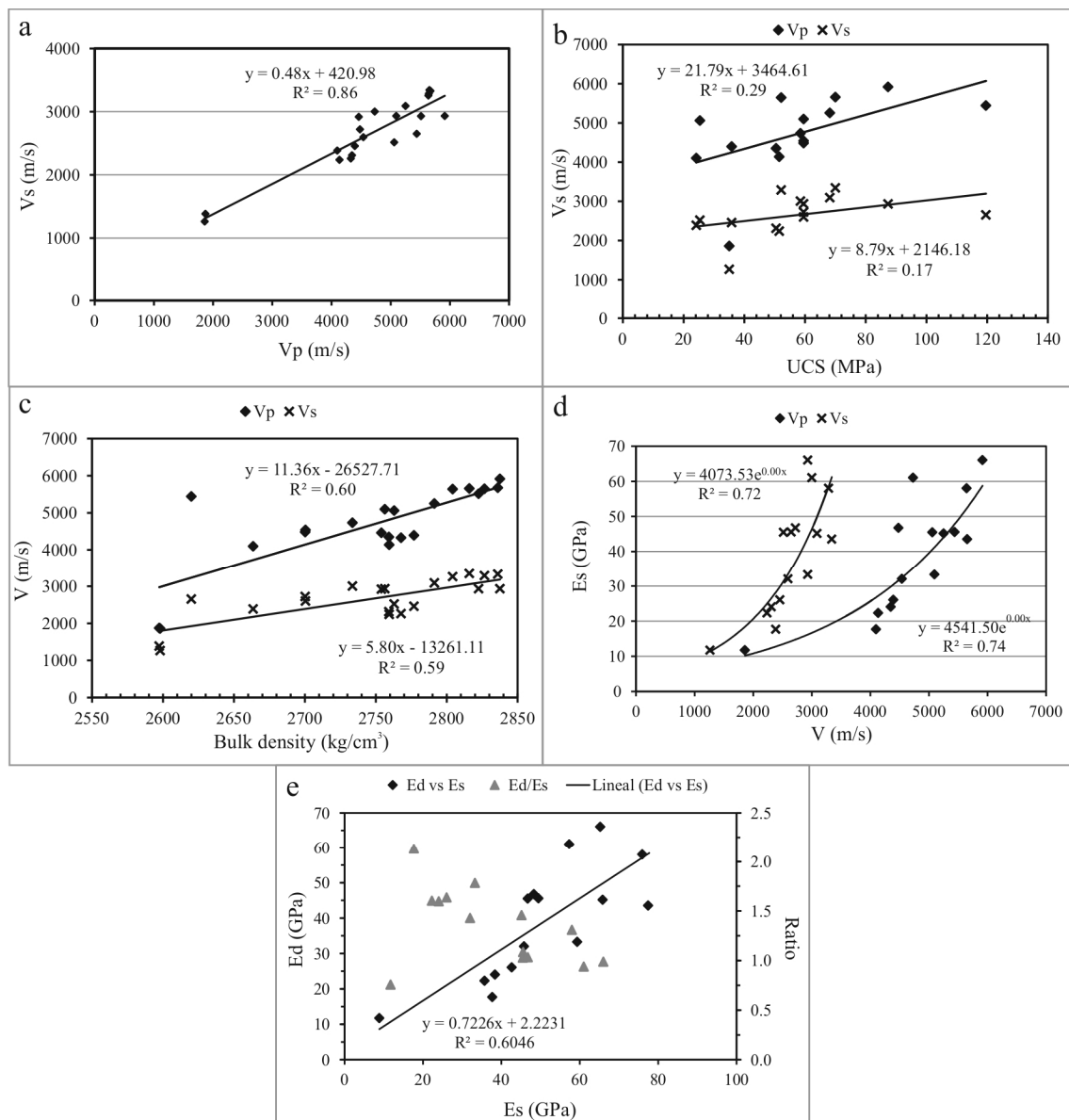


Figure 14. Correlation between propagation velocities of ultrasonic wave and other parameters: (a) V_p and V_s ; (b) V_p and V_s with UCS; (c) V_p and V_s with bulk density; (d) V_p and V_s with static modulus E_s ; (e) Elastic modulus ratio.

Because careful petrographic studies showed the existence of some mineral fibers in these rocks, corresponding to chrysotile, and because the increasing awareness regarding the content of asbestos in quarrying materials, we analyzed extra samples from the same quarries by SEM to clarify the major component of the serpentine phases in the rocks from Moeche. The preliminary results are compatible with all the analytical methods used to characterize the studied serpentinites: SEM shows that the major serpentine phase is antigorite (Figure 15). A small percentage is shown as lizardite, and very few

fibers of chrysotile were detected, but in a small amount that could be compatible with the potential extraction of the stone. Further studies on this subject are being carried out to study the safe handling of a potential re-opening.

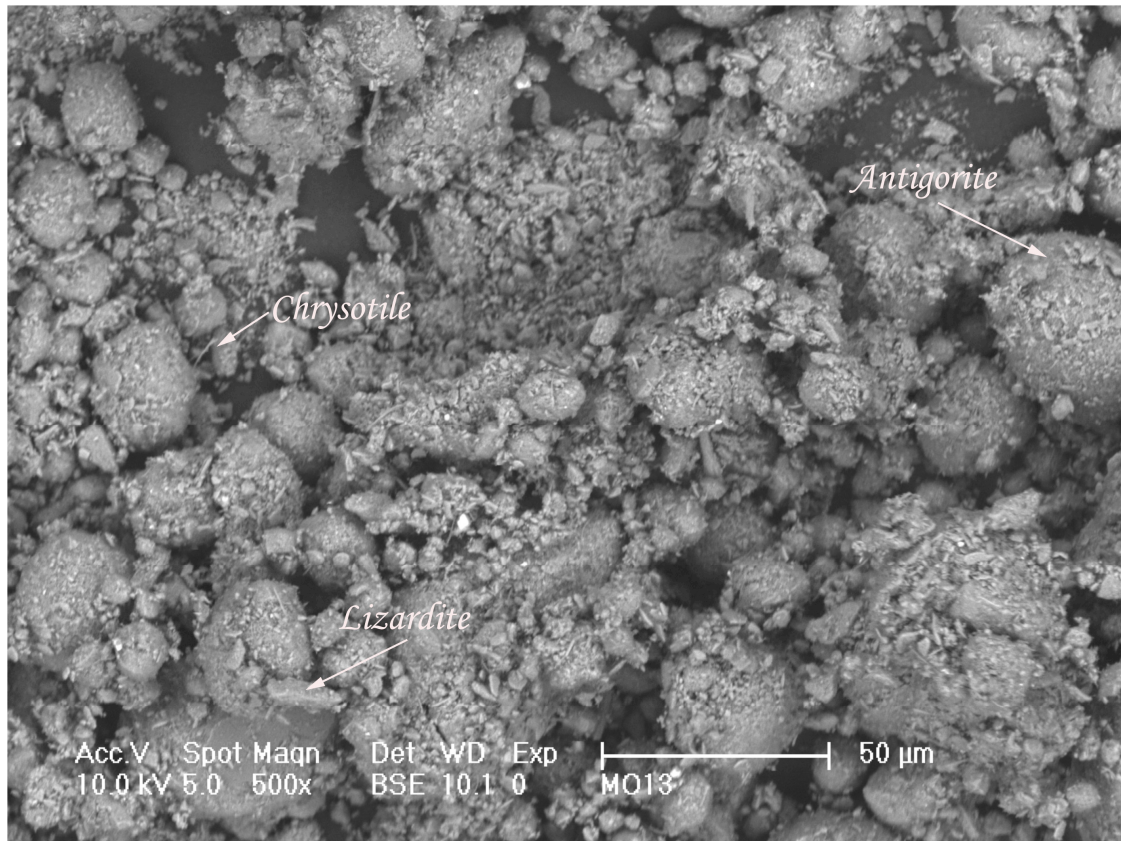


Figure 15. Scanning electron micrograph of a serpentinite sample from Moeche. There are predominant globular morphologies identified as antigorite, which is in agreement with the x-ray diffraction analysis. The few prismatic shapes correspond to lizardite crystals, and also a few particles with acicular shapes observed in the micrographs are assigned to the chrysotile phase of the serpentine [55].

6. Conclusions

Serpentinites from Moeche are very heterogeneous rocks. It is difficult to establish relatively well-defined intervals for their mechanical properties. They are rocks whose strengths range from weak to very strong, and this property seems to be reflected by the textural appearance of the rock. It is confirmed that in most cases, and in contrast to the initial general idea, the most resistant samples are those with a more brecciated aspect. This type of sample has significant carbonation that progresses, in conjunction with talc, through a network of irregular fractures, some of them coinciding with the foliation of the rock, but having poor continuity. Strongly-carbonated rocks are of interest for the potential conservation-restoration of architectural heritage that used that stone, locally named as “Pedra de Toelo” or “Pedra de Moeche”.

Continuous and persistent foliation weakens these rocks, even when detected only at a microscopic scale.

The bulk density of the Moeche serpentinites does not correlate with either the UCS or the velocity of ultrasonic waves, and hence they cannot be recommended for indirect estimations. However, ultrasonic data can be useful for obtaining a first approach to the static elastic parameters, which are usually lower than the dynamic parameters, the E_d/E_s ratio increases with E_d .

The general trend observed in previous studies addressing serpentinites from other locations cannot be confirmed in the Moeche serpentinites, but, similar to the carbonated serpentinites from

Macael (SE Spain), the higher the percentage of carbonates, the lower the UCS. In any case, it seems that carbonates govern the fracture morphology. What might possibly further determine the UCS in the serpentinites from Moeche is their origin; the UCS increases if there is a carbonate replacement of serpentine phases, and decreases if carbonate has filled the fractures.

A direct relationship between the mineralogical composition and the compressive strength of these rocks has not been determined. Nevertheless, a general tendency of the latter to be higher when the proportion of serpentines is also higher can be observed.

The complex relationship between mineralogy, structure, and microstructure is responsible for the large spread of values of resistance of these rocks, which in turn makes it difficult to establish a threshold value for gauging its suitability as a dimension stone based on this property. For such thresholds, these rocks do not meet American standards (ASTM), owing to their high water absorption and their low minimum UCS, which is in agreement with serpentinites from other currently operating quarries. Consequently, a draft outlining the European standards for these rocks is necessary and should include, among others, the petrographic characteristics of the rock and its mineral composition, both of which are factors that, according to the results obtained in this study, determine the geomechanical behavior of serpentinites.

According to the study presented in this paper, the serpentinites from Moeche need a complete and specific mineralogical, physical, and mechanical characterization before they can be used properly, as an ornamental stone or as conservation-restoration material, to avoid undesirable results for construction and conservation-restoration activities. Preliminary positive results associated to our research are related to the very low content of asbestos, in any of the possible phases of amphibole or chrysotile, detected in these rocks, which is an advantage in terms of quarrying even for further testing.

The present paper will be a step forward in the preservation of cultural and architectonic heritage of Galicia.

Author Contributions: J.N., R.N., S.M. and D.P. were responsible for the conceptualization and validation of data, as well as for the writing and editing of the manuscript. All authors were involved in sampling. D.P. was responsible for the funding acquisition.

Funding: This research was funded by the projects: CGL2004–03048, CGL2006–05128/BTE and BIA2017-85897-R from the Spanish government, and the University of Salamanca through project TCUE 2015 and the University's own financial program.

Acknowledgments: The authors wish to thank the Laboratory of Applied Petrology of the CSIC-University of Alicante Associated Unit for their help with the ultrasonic tests, and the Language Services of the University of Salamanca for the language revision. D. Pereira acknowledges the research teams of Inorganic Geochemistry of the universities of Salamanca and Complutense of Madrid for SEM analysis and discussion of results. Two anonymous reviewers are acknowledged for their help in improving this paper.

Conflicts of Interest: The authors declare no conflict of interest. The funders had no role in the design of the study, analyses, or interpretation of data; in the writing of the manuscript, or in the decision to publish the results.

References

1. O'Hanley, D.S. *Serpentinites: Records of Tectonic and Petrological History*; Oxford University Press: New York, NY, USA, 1996; p. 277.
2. Meierding, T.C. Weathering of serpentine stone buildings in the Philadelphia region: a geographic approach related to acidic deposition. In *Stone Decay in the Architectural Environment*; Turkington, A.V., Ed.; Geological Society of America: Denver, CO, USA, 2005; Volume 399, pp. 17–25. [[CrossRef](#)]
3. Pereira, M.D.; Peinado, M.; Yenes, M.; Monterrubio, S.; Nespereira, J.; Blanco, J.A. Serpentinites from Cabo Ortegal (Galicia, Spain): A search for correct use as ornamental stones. In *Natural Stone Resources for Historical Monuments*; Prikryl, R., Török, A., Eds.; Geological Society: London, UK, 2010; Volume 333, pp. 81–85.
4. Navarro, R.; Pereira, D.; Rodríguez-Navarro, C.; Sebastian-Pardo, E. The Sierra Nevada serpentinites: The serpentinites most used in Spanish heritage buildings. In *Global Heritage Stone: Towards International Recognition of Building and Ornamental Stones*; Pereira, D., Marker, B., Kramar, S., Cooper, B., Schouenborg, B., Eds.; Geological Society: London, UK, 2015; Volume 407, pp. 101–108.

5. Pereira, M.D.; Blanco, J.A.; Peinado, M. Study on Serpentinities and the consequence of the misuse of natural stone in buildings for construction. *J. Mater. Civ. Eng.* **2013**, *25*, 1563–1567. [[CrossRef](#)]
6. Navarro, R.; Pereira, D.; Gimeno, A.; Del Barrio, S. Influence of natural carbonation process in serpentinites used as construction and building materials. *Constr. Build. Mater.* **2018**, *170*, 537–546. [[CrossRef](#)]
7. Coumantakis, J. Comportement des peridotites et des serpentinites de la grece en travaux publics et leur proprietes physiques et mecaniques. *Bull. Eng. Geol. Environ.* **1982**, *25*, 53–60. [[CrossRef](#)]
8. Glawe, U.; Upreti, B. Better understanding of the strengths of serpentinite bimrock and homogeneous serpentinite. *Felsbau Rock Soil Eng.* **2004**, *22*, 53–60.
9. Ozsoy, E.A.; Yilmaz, G.; Arman, H. Physical, mechanical and mineralogical properties of ophiolitic rocks at the Yakakayi dam site, Eskisehir, Turkey. *Sci. Res. Essays* **2010**, *5*, 2579–2587.
10. Marinos, P.; Hoek, E.; Marinos, V. Variability of the engineering properties of rock masses quantified by the geological strength index: The case of ophiolites with special emphasis on tunnelling. *Bull. Eng. Geol. Environ.* **2005**, *65*, 129–142. [[CrossRef](#)]
11. Christensen, N.I. Serpentinities, peridotites, and seismology. *Int. Geol. Rev.* **2004**, *46*, 795–816. [[CrossRef](#)]
12. Ismael, I.; Hassan, M. Characterization of some Egyptian serpentinites used as ornamental stones. *Chin. J. Geochem.* **2008**, *27*, 140–149. [[CrossRef](#)]
13. Diamantis, K.; Gartzos, E.; Migiros, G. Study on uniaxial compressive strength, point load strength index, dynamic and physical properties of serpentinites from central Greece: Test results and empirical relations. *Eng. Geol.* **2009**, *108*, 199–207. [[CrossRef](#)]
14. Kurtulus, C.; Bozkurt, A.; Endes, H. Physical and mechanical properties of serpentinitized ultrabasic rocks in NW Turkey. *Pure Appl. Geophys.* **2012**, *169*, 1205–1215. [[CrossRef](#)]
15. Navarro, R.; Pereira, M.D.; Gimeno, A.; Del Barrio, S. Verde Macael: A serpentinite wrongly referred to as a marble. *Geoscience* **2013**, *3*, 102–113. [[CrossRef](#)]
16. Navarro, R.; Pereira, D.; Gimeno, A.; del Barrio, S. Characterization of the natural variability of Macael serpentinite (Verde Macael) (Almería, south of Spain) for their appropriate use in the building industry. In *Engineering Geology for Society and Territory. Volume 5: Urban Geology, Sustainable Planning and Landscape Exploitation*; Lollino, G., Manconi, A., Guzzetti, F., Culshaw, M., Bobrowsky, P., Luino, F., Eds.; Springer International Publishing AG: Cham, Switzerland, 2015; Volume 5, pp. 209–211.
17. Burgoa-Fernández, J.J. El patrimonio etnográfico y el arte popular: cruceros y petos de ánimas de los municipios de Moeche y San Sadurniño. *Anuario Brigantino* **2000**, *23*, 477–494.
18. Pereira, M.D.; Blanco, J.A.; Yenes, M.; Peinado, M. Las serpentinitas y su correcta utilización en construcción. *Roc Maquina* **2005**, *9*, 24–27.
19. Pereira, M.D.; Peinado, M.; Blanco, J.A.; Yenes, M. Geochemical characterization of serpentinites at Cabo Ortegal, northwestern Spain. *Can. Mineral.* **2008**, *46*, 317–327. [[CrossRef](#)]
20. Blanco, J.; Peinado, M.; Pereira, D.; Yenes, M.; Nespereira, J.; Monterrubio, S. Mineralogy of serpentinites: A clue for their use as ornamental stones. *Geophys. Res. Abstr.* **2007**, *9*, 05494.
21. ASTM. *C-1526-02 Standard Specification for Serpentine Dimension Stone*; American Society for Testing and Materials International: Pennsylvania, PA, USA, 2002; p. 2.
22. Matte, P. The Variscan collage and orogeny (480–290 Ma) and the tectonic definition of the Armorica microplate: A review. *Terra Nova* **2003**, *13*, 122–128. [[CrossRef](#)]
23. Arenas, R.; Martínez-Catalán, J.R.; Sánchez-Martínez, S.; Díaz-García, F.; Abati, J.; Fernández-Suárez, J.; Andonaegui, P.; Gómez-Barreiro, J. Paleozoic ophiolites in the Variscan suture of Galicia (northwest Spain): Distribution, characteristics, and meaning. In *4-D Framework of Continental Crust*; Hatcher, J.R.D., Carlson, M.P., McBride, J.H., Martínez-Catalán, J.R., Eds.; Geological Society of America: Denver, CO, USA, 2007; Volume 200, pp. 425–444.
24. Arenas, R.; Sánchez-Martínez, S.; Castiñeiras, P.; Jeffries, T.E.; Díez-Fernández, R.; Andonaegui, P. The basal tectonic mélange of the Cabo Ortegal Complex (NW Iberian Massif): A key unit in the suture of Pangea. *J. Iberian Geol.* **2009**, *35*, 85–125.
25. Albert, R.; Arenas, R.; Sánchez-Martínez, S.; Gerdes, A. The eclogite facies gneisses of the Cabo Ortegal Complex (NW Iberian Massif): Tectonothermal evolution and exhumation model. *J. Iberian Geol.* **2012**, *38*, 389–406. [[CrossRef](#)]
26. Ordóñez-Casado, B.; Gebauer, D.; Schäfer, H.J.; Gil Ibarguchi, J.I.; Peucat, J.J. A single Devonian subduction event for the HP/HT metamorphism of the Cabo Ortegal complex within the Iberian Massif. *Tectonophysics* **2001**, *332*, 359–385. [[CrossRef](#)]

27. Mendia, M.; Ibaguchi, J.I. Petrografía y condiciones de formación de las rocas ultramáficas con granate asociadas a las eclogitas de Cabo Ortegal. *Geogaceta* **2005**, *37*, 31–34.
28. Hawkins, A.B. Aspects of rock strength. *Bull. Eng. Geol. Environ.* **1998**, *57*, 17–30. [[CrossRef](#)]
29. Benavente, D.; Martínez-Martínez, J.; Jáuregui, P.; Rodríguez, M.A.; García del Cura, M.A. Assessment of the strength of building rocks using signal processing procedures. *Constr. Build. Mater.* **2006**, *20*, 562–568. [[CrossRef](#)]
30. AENOR. *Geotecnia: ensayos de campo y de laboratorio*; Asociación Española De Normalización Y Certificación: Madrid, Spain, 1999; p. 385.
31. Rietveld, H.M. A profile refinement method for nuclear and magnetic structures. *J. Appl. Crystallogr.* **1969**, *2*, 65–71. [[CrossRef](#)]
32. ASTM. *C1721-15 Standard Guide for Petrographic Examination of Dimension Stone*; American Society for Testing and Materials International: Pennsylvania, PA, USA, 2015; p. 2.
33. Jaeger, J.C. Shear failure of anisotropic rock. *Geol. Mag.* **1960**, *97*, 65–72. [[CrossRef](#)]
34. Wicks, F.J.; Whittaker, E.J.W. Serpentine textures and serpentinization. *Can. Mineral.* **1977**, *15*, 459–488.
35. Donath, F.A. Strength variation and deformational behaviour of anisotropic rocks. In *State of Stress in the Earth's Crust*; Judd, W.R., Ed.; Elsevier: New York, NY, USA, 1964; pp. 281–298.
36. Hoek, E. Fracture of anisotropic rock. *J. South. Afr. Inst. Min. Metall.* **1964**, *64*, 510–518.
37. Singh, J.; Ramamurthy, T.; Venkatappa Rao, G. Strength anisotropies in rocks. *Ind. Geotech. J.* **1989**, *19*, 147–166.
38. Ramamurthy, T. Strength, modulus responses of anisotropic rocks. In *Comprehensive Rock Engineering*; Hutson, J.A., Ed.; Pergamon: Oxford, UK, 1993; Volume 1, pp. 313–329.
39. ISRM. Rock characterization. Testing and monitoring. In *Suggested Methods Prepared by the Commission on Testing Methods*; Brown, E.T., Ed.; International Society for Rock Mechanics; ISRM Turkish National Group; Pergamon Press: Ankara, Turkey, 1981; p. 221.
40. Deere, D.U.; Miller, R.P. *Engineering Classification and Index Properties for Intact Rock*; U.S. Air Force Systems Command Air Force Weapons Lab.: Kirtland Air Force Base, NM, USA, 1966; p. 324.
41. Pereira, M.D.; Neves, L.; Pereira, A.; González-Neila, C. Natural radioactivity in ornamental stones: An approach to its study using stones from Iberia. *Bull. Eng. Geol. Environ.* **2011**, *70*, 543–547. [[CrossRef](#)]
42. Benavente, D. Propiedades físicas y utilización de rocas ornamentales. In *Utilización de Rocas y Minerales Industriales. Seminarios de la Sociedad Española de Mineralogía*; García del Cura, M.A., Cañaveras, J.C., Eds.; Sociedad Española de Mineralogía: Madrid, Spain, 2006; Volume 2, pp. 123–153.
43. Romana, M.; Vásárhelyi, B. A Discussion on the decrease of unconfined compressive strength between saturated and dry rock samples. In Proceedings of the 11th ISRM Congress, Lisbon, Portugal, 9–13 July 2007.
44. Siegesmund, S.; Dürrast, H. Physical and mechanical properties of rocks. In *Stone in Architecture: Properties, Durability*, 4th ed.; Siegesmund, S., Snethlage, R., Eds.; Springer: Berlin, Germany, 2011; pp. 97–225.
45. Kahraman, S. Evaluation of simple methods for assessing the uniaxial compressive strength of rock. *Int. J. Rock Mech. Min. Sci.* **2001**, *38*, 981–994. [[CrossRef](#)]
46. Tsiambaos, G.; Sabatakakis, N. Considerations on strength of intact sedimentary rocks. *Eng. Geol.* **2004**, *72*, 261–273. [[CrossRef](#)]
47. Sonmez, H.; Gokceoglu, C.; Medley, E.W.; Tuncay, E.; Nefeslioglu, H.A. Estimating the uniaxial compressive strength of a volcanic bimrock. *Int. J. Rock Mech. Min. Sci.* **2006**, *43*, 554–561. [[CrossRef](#)]
48. Yesiloglu-Gultekin, N.; Gokceoglu, C.; Sezer, E.A. Prediction of uniaxial compressive strength of granitic rocks by various nonlinear tools and comparison of their performance. *Int. J. Rock Mech. Min. Sci.* **2013**, *62*. [[CrossRef](#)]
49. Nespereira, J.; Blanco, J.A.; Yenes, M.; Pereira, D. Irregular silica cementation in sandstones and its implication on the usability as building stone. *Eng. Geol.* **2010**, *115*, 167–174. [[CrossRef](#)]
50. Ulusay, R.; Türel, K.; Ider, M.H. Prediction of engineering properties of a selected litharenite sandstone from its petrographic characteristics using correlation and multivariate statistical techniques. *Eng. Geol.* **1994**, *38*, 135–157. [[CrossRef](#)]
51. Moos, D.; Pezard, P.A. Relationships between strengths and physical properties of samples recovered during Legs 137, 140, and 148 from Hole 504B. In *Proceedings ODP, Scientific Results*; Alt, J.C., Kinoshita, H., Stokking, L.B., Michael, P.J., Eds.; Ocean Drilling Program: College Station, TX, USA, 1996; Volume 148, pp. 401–407.

52. Gupta, A.S.; Seshagiri Rao, K. Weathering effects on the strength and deformational behaviour of crystalline rocks under uniaxial compression state. *Eng. Geol.* **2000**, *56*, 257–274. [[CrossRef](#)]
53. Martínez-Martínez, J.; Benavente, D.; García del Cura, M.A. Comparison of the static and dynamic elastic modulus in carbonate rocks. *Bull. Eng. Geol. Environ.* **2011**, *71*, 263–268. [[CrossRef](#)]
54. Al-Shayea, N.A. Effects of testing methods and conditions on the elastic properties of limestone rock. *Eng. Geol.* **2004**, *74*, 139–156. [[CrossRef](#)]
55. Cressey, B.A.; Whittaker, E.J.W. Five-fold symmetry in chrysotile asbestos revealed by transmission electron microscopy. *Mineral. Mag.* **1993**, *5*, 729–732. [[CrossRef](#)]



© 2019 by the authors. Licensee MDPI, Basel, Switzerland. This article is an open access article distributed under the terms and conditions of the Creative Commons Attribution (CC BY) license (<http://creativecommons.org/licenses/by/4.0/>).